

**ADA 278605**

Final Technical Report for:

**HIGH TEMPERATURE HETEROJUNCTION BIPOLAR TRANSISTORS**

Submitted under:

Contract Number DAAH04-93-C-0040

Contract period:

1 September 1993 through 28 February 1994

Report period:

1 September 1993 through 28 February 1994

Submitted to:

U.S. Army Research Office

P.O. Box 12211

Research Triangle Park, NC 27709-2211

Submitted by:

H. Paul Maruska, Ph.D.

Spire Corporation

One Patriots Park

Bedford, MA 01730-2396

QUAN . . . . . 3

REPORT DOCUMENTATION PAGE			Form Approved OMB No. 0704-0188	
Public reporting burden for this collection of information is estimated to average 1 hour per response, including the time for reviewing instructions, searching existing data sources, gathering and maintaining the data needed, and completing and reviewing the collection of information. Send comments regarding this burden estimate or any other aspect of this collection of information, including suggestions for reducing this burden, to Washington Headquarters Services, Directorate for Information Operations and Reports, 1215 Jefferson Davis Highway, Suite 1204, Arlington, VA 22202-4302, and to the Office of Management and Budget, Paperwork Reduction Project (0704-0188), Washington, DC 20503				
1. AGENCY USE ONLY (Leave blank)		2. REPORT DATE 15 Apr 94		3. REPORT TYPE AND DATES COVERED Final Technical, 1/9/93-2/28/94
4. TITLE AND SUBTITLE High Temperature Heterojunction Bipolar Transistors			5. FUNDING NUMBERS	
6. AUTHOR(S) H. Paul Maruska, Ph.D.				
7. PERFORMING ORGANIZATION NAME(S) AND ADDRESS(ES) Spire Corporation One Patriots Park Bedford, MA 01730-2396			8. PERFORMING ORGANIZATION REPORT NUMBER  FR-60296	
9. SPONSORING/MONITORING AGENCY NAME(S) AND ADDRESS(ES) U.S. Army Research Office P. O. Box 12211 Research Triangle Park, NC 27709-2211			10. SPONSORING/MONITORING AGENCY REPORT NUMBER  CLIN 002AA	
11. SUPPLEMENTARY NOTES The view, opinions and/or findings contained in this report are those of the author(s) and should not be construed as an official Department of the Army position, policy, or decision, unless so designated by other documentation.				
12a. DISTRIBUTION/AVAILABILITY STATEMENT  Approved for public release; distribution unlimited			12b. DISTRIBUTION CODE  A	
13. ABSTRACT (Maximum 200 words)  The program objective was to develop deposition conditions for wide bandgap nitride semiconductors consistent with the requirements for either bipolar junction transistors or field effect transistors that can function at high speed in environments having elevated temperatures. The fundamental material for these studies was gallium nitride. We proceeded to define crystal growth parameters for preparing epitaxial thin films of $\text{In}_x\text{Ga}_{1-x}\text{N}$ alloys which feature smaller bandgaps than GaN. To grow the nitride alloys, we used a modified metalorganic chemical vapor deposition (MOCVD) reactor which provided activated nitrogen generated as an electron cyclotron resonance microwave plasma. Samples were successfully prepared with compositions throughout the alloy series, viz, with bandgaps ranging from 1.9 eV (InN) to 3.4 eV (GaN). The films were transparent with specular surfaces, and X-ray diffraction studies showed the GaN was single crystalline with the c-axis perpendicular to the substrate. The nitride alloys varied in color from deep red to yellow. We believe that is the first report of preparing $\text{In}_x\text{Ga}_{1-x}\text{N}$ alloys in a plasma assisted MOCVD reactor. Because we can vary the bandgap of $\text{In}_x\text{Ga}_{1-x}\text{N}$ as desired, we can control the potential barrier between the base and emitter in a heterojunction bipolar transistor, or the spacer and the channel in a high electron mobility field effect transistor.				
14. SUBJECT TERMS  bipolar junction transistor, high temperature, ECR plasma, nitride MOCVD			15. NUMBER OF PAGES 27	
			16. PRICE CODE	
17. SECURITY CLASSIFICATION OF REPORT  Unclassified	18. SECURITY CLASSIFICATION OF THIS PAGE  Unclassified	19. SECURITY CLASSIFICATION OF ABSTRACT  Unclassified	20. LIMITATION OF ABSTRACT  Unlimited	

# TABLE OF CONTENTS

	<u>Page</u>
1 SUMMARY .....	1
2 INTRODUCTION .....	2
2.1 Background for Preparation and Properties of Semiconducting Nitrides ...	2
2.2 High Temperature Transistors .....	4
2.3 Alternative Nitride Materials for Transistor Applications .....	5
2.4 Plasma Assisted Deposition of Nitrides .....	7
3 EXPERIMENTAL RESULTS AND DISCUSSION .....	8
3.1 Development of ECR-Plasma Assisted MOCVD of Nitrides .....	8
3.2 Experimental Conditions for GaN Deposition .....	9
3.3 Properties of GaN Films .....	10
3.4 Development of ECR-Plasma Assisted MOCVD of Indium Nitride .....	13
3.5 Optical Absorption Studies .....	17
3.6 Summary of Initial Work on Standard MOCVD of GaN .....	17
3.6.1 Basic Growth Parameters .....	17
3.6.2 GaN Crystal Growth .....	18
3.6.3 GaN Characterization .....	18
4 ANALYSIS OF RESULTS AND RECOMMENDATIONS .....	20
5 REFERENCES .....	21

Accession For	
NTIS	CRAB
DTIC	TAB
Unannounced	
Justification	
By	
Distribution /	
Availability	
Dist	Avail and/or Special
A-1	

## LIST OF ILLUSTRATIONS

		<u>Page</u>
1	Squared variation of the absorption coefficient as a function of photon energy for GaN-InN alloys prepared by PA-MOCVD .....	2
2	Bandgap energy vs. molar fraction for InN-GaN and AlN-GaN alloys .....	3
3	Spire's concept of a high temperature HBT based on GaN-InN alloys .....	5
4	Plan and cross-sectional view of fabricated HEMT .....	6
5	Spire's ECR plasma source modified as a crystal growth reactor .....	8
6	Showerhead gas injector .....	10
7	X-ray diffraction pattern of plasma assisted GaN, indicating an epitaxial single crystalline film .....	11
8	Absorption spectrum of plasma assisted GaN film, showing sharp absorption edge at 365 nm .....	12
9	Photomicrograph of the surface of a GaN film prepared in the plasma assisted MOCVD reactor .....	12
10	Growth of InN by PA-MOCVD: better films result at larger N/TMI flow ratio ..	14
11	High growth temperatures apparently pyrolyze the TMI, introducing carbon contaminants .....	14
12	Auger electron spectroscopy of InN film .....	15
13	Varying Ga:In ratio shifts the absorption band edge .....	16
14	Auger electron spectroscopy of $\text{In}_x\text{Ga}_{1-x}\text{N}$ film .....	16
15	Optical transmission spectrum of GaN sample grown by conventional MOCVD .	19
16	Auger analysis of GaN sample .....	20
17	X-ray diffraction analysis of GaN sample #11, indicating (101) peak of GaN ...	20

## LIST OF TABLES

	<u>Page</u>
I    Growth conditions for ECR plasma assisted MOCVD of GaN . . . . .	11
II    Growth conditions for ECR plasma assisted MOCVD of InN and $\text{In}_x\text{Ga}_{1-x}\text{N}$ . . . .	13

## 1 SUMMARY

The objective of this program was to develop deposition conditions for wide bandgap nitride semiconductors consistent with the requirements for either bipolar junction transistors or field effect transistors that can function at high speed in environments having elevated temperatures. The fundamental material for these studies has been gallium nitride, a semiconductor with a bandgap of 3.4 eV. A nitride with a smaller bandgap would provide a potential barrier required for controlling the direction of current flow in the device. Consequently the major thrust of the program has centered on defining deposition parameters for preparing epitaxial thin films of smaller bandgap nitrides to form heterojunctions with GaN. Such a narrower bandgap nitride film could function as the base of a high operating temperature heterojunction bipolar transistor (HBT), or as the channel in a high electron mobility field effect transistor (HEMT).

The two most promising nitride materials with bandgaps smaller than GaN are  $\text{Zn}_{0.5}\text{Ge}_{0.5}\text{N}$  and the alloy series  $\text{In}_x\text{Ga}_{1-x}\text{N}$ . We have decided that since the  $\text{In}_x\text{Ga}_{1-x}\text{N}$  alloy series allows a wide range of choices of bandgaps, and hence variable potential barriers, it is more beneficial to pursue the growth of these alloys rather than the stoichiometric compound  $\text{Zn}_{0.5}\text{Ge}_{0.5}\text{N}$ . Additionally, with  $\text{Zn}_{0.5}\text{Ge}_{0.5}\text{N}$ , we would be faced with possible complications in defining growth parameters due to the probable precipitation of second phases such as  $\text{Zn}_3\text{N}_2$  or  $\text{Ge}_3\text{N}_4$  under certain unoptimized conditions. Therefore, all work constituted the definition of deposition conditions for producing  $\text{In}_x\text{Ga}_{1-x}\text{N}$  alloys using a plasma source of nitrogen.

Samples have been prepared with compositions throughout the alloy series, viz, with bandgaps ranging from 1.9 eV (InN) to 3.4 eV (GaN). Figure 1 shows the square of the absorption constant vs. energy for four of our samples, viz., InN, GaN, and two intermediary alloys. The straight line fits to the measured data are consistent with the optical properties of direct bandgap semiconductors,<sup>1</sup> and the intersections of the straight lines with the energy axis yield the proper bandgaps for InN and GaN.<sup>2</sup> Therefore, the first materials phase of the program has proven to be highly successful.

At the start of the program we relied on a standard reactor based on a horizontal tube design using trimethylgallium and ammonia as the reactants. Because results for the GaN films prepared in this reactor did not prove to be very promising, we proceeded to the main objective of the program, which was to modify an alternative reactor to include a more reactive nitrogen specie. We subsequently succeeded in developing conditions for depositing GaN, InN, and  $\text{In}_x\text{Ga}_{1-x}\text{N}$  in a modified metalorganic chemical vapor deposition (MOCVD) reactor. We modified the reactor to include a more reactive nitrogen specie, which was accomplished by creating a nitrogen plasma. The activated nitrogen is generated as an electron cyclotron resonance (ECR) microwave plasma. Therefore, we are now operating a new plasma assisted MOCVD reactor, hereafter referred to as a PA-MOCVD reactor.

We used trimethylgallium (TMG) as the gallium source, and added trimethylindium (TMI) as the indium source for our PA-MOCVD reactor. Two inch diameter sapphire wafers, epi grade polish, having the (0001) orientation, were cut into 1 cm squares. These served as substrates for the program. We first successfully deposited films of GaN which were smooth and transparent, and InN films which are, as expected, dark orange in color. We then concentrated on producing  $\text{In}_x\text{Ga}_{1-x}\text{N}$  alloys.

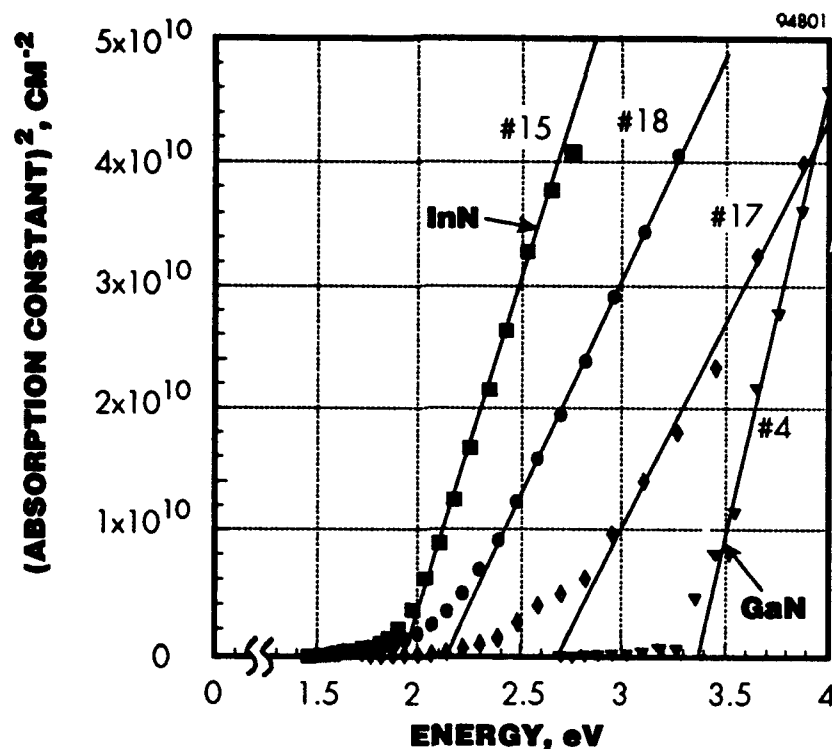


**Figure 1** *Squared variation of the absorption coefficient as a function of photon energy for GaN-InN alloys prepared by PA-MOCVD.*

Nine experimental runs for growing GaN were made once the reactor was placed in operation, and after several parameters were adjusted, high quality films of GaN were produced. The films were transparent with specular surfaces, and X-ray diffraction studies showed the best one to be a single crystal oriented with the c-axis perpendicular to the substrate. We then progressed to determining conditions for depositing films of InN. Most significantly, we have succeeded in producing  $\text{In}_x\text{Ga}_{1-x}\text{N}$  alloys which exhibited bandgaps intermediate between InN (1.9 eV) and GaN (3.4 eV). We believe that is the first report of preparing  $\text{In}_x\text{Ga}_{1-x}\text{N}$  alloys in a plasma assisted MOCVD reactor. Because we can vary the bandgap of  $\text{In}_x\text{Ga}_{1-x}\text{N}$ , we are in a position to control the potential barrier between the base and emitter in an HBT, or the spacer and the channel in a HEMT. Let us also note that the band edges of the films shown in Figure 1 would correspond to red, green, blue, and ultraviolet light emission if the samples were fabricated into light-emitting diodes.

## 2 INTRODUCTION

### 2.1 Background for Preparation and Properties of Semiconducting Nitrides

The III-V compound semiconductors indium nitride (InN), gallium nitride (GaN), and aluminum nitride (AlN) are completely mutually soluble, and their alloys exhibit bandgaps spanning the range of 1.9 eV (650 nm) to 6.2 eV (200 nm) (Figure 2). Clearly, this entire alloy series of the nitrides is of great interest for providing displays (*e.g.*, light-emitting diodes), transistors for high temperature operation, as well as optical filters which rely on their strong optical absorption characteristics.

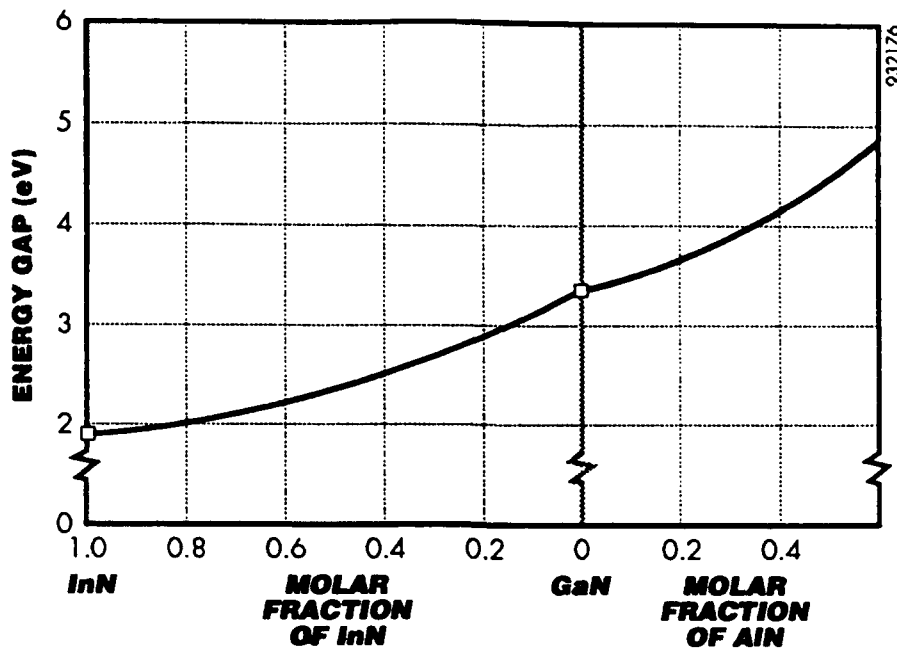


**Figure 2** *Bandgap energy vs. molar fraction for InN-GaN and AlN-GaN alloys.*

Gallium nitride is the most commonly studied wide bandgap semiconductor; it was first prepared as a single crystal epitaxial film in 1969 by Maruska.<sup>3</sup> With a bandgap of 3.4 eV, the material is basically not affected by generation of intrinsic carriers at ambient temperatures of several hundred degrees celsius, and should function properly up to 600°C or higher. Therefore it has great potential for the development of high temperature transistors. Thus GaN transistors will find applications in avionics, spacecraft, automotive engine control, monitoring of power plants and nuclear reactors, and characterization of oil wells.

Furthermore, the large bandgap results in a much larger value of reverse breakdown voltage in junction devices when compared with silicon transistors doped with comparable concentrations of impurities. For a given breakdown voltage, therefore, GaN devices can be produced with much higher doping concentrations than would be allowed for silicon, meaning that their power handling capabilities are greatly enhanced. In addition, GaN has a lower dielectric constant than Si, which should allow devices to operate at higher frequencies. Finally, the transparent nature of GaN means that it would not be affected to illumination from room lighting.

Maruska's original technology for growing crystalline films of GaN was based upon the surface reaction on sapphire ( $\text{Al}_2\text{O}_3$ ) substrates between vapors of  $\text{GaCl}_3$  and  $\text{NH}_3$  in a hot walled reactor.<sup>3</sup> Maruska used (0001) oriented sapphire wafers, and determined that GaN crystallizes in the hexagonal wurtzite structure with lattice parameters  $a = 3.189$  and  $c = 5.185$ . He showed that GaN has a direct bandgap of 3.39 eV, and all of his films were n-type with carrier concentrations as high as  $1 \times 10^{20} \text{ cm}^{-3}$ . He and his colleagues performed extensive



characterization studies on this material,<sup>4,5</sup> and suggested that the high intrinsic carrier concentration was a result of nitrogen vacancies formed during the growth. Maruska found that the dopants Zn and Mg act as deep acceptors in GaN,<sup>6</sup> and formed m-i-n diodes which emitted blue and violet light.<sup>7</sup> Finally, Maruska developed the model for electroluminescence in GaN m-i-n diodes based on impact ionization of luminescence centers.<sup>8</sup>

More recently, there have been several reports of the preparation of GaN by metalorganic chemical vapor deposition (MOCVD).<sup>9,10,11</sup> By careful control of the deposition process, carrier concentration levels have been reduced to the  $10^{18} \text{ cm}^{-3}$  range. However, nitrogen vacancies apparently continue to pose a problem. A more active source of nitrogen to replace ammonia holds the promise of alleviating the nitrogen vacancy problem.

## 2.2 High Temperature Transistors

It is well known that there are basically two classes of transistors, bipolar junction transistors and field effect transistors. There is much current interest in applying wide bandgap materials like GaN to both types of structures. For a bipolar transistor, the simplest approach would be to construct a stack of npn or pnp doped layers of GaN, to form an emitter, base, and collector. However, it is known that the gain of any bipolar transistor is limited by the back injection of minority carriers from the base into the emitter, and therefore the ability to prepare a *heterojunction bipolar transistor* is an important materials research endeavor for the III-V nitride family.<sup>12</sup> In a heterojunction bipolar transistor (HBT), the emitter material is chosen to have a wider bandgap than the base,<sup>13</sup> thus limiting the deleterious injection of carriers from the base back into the emitter. Therefore, it would be useful to find a material which is closely lattice matched to GaN, but which offers a slightly smaller bandgap, to function as the base. Our concept of a high temperature heterojunction bipolar transistor utilizing GaN for the emitter and collector and an  $\text{In}_x\text{Ga}_{1-x}\text{N}$  alloy for the base is shown in Figure 3.

Because bipolar junction transistors are minority carrier devices, it appears there may be some difficulties with such structures in emerging materials like GaN, which tend to have crystalline defects that can reduce the minority carrier lifetime. Furthermore, p-type doping has only recently been announced in GaN,<sup>14</sup> and p-type conductivity had to be induced by irradiating Mg-doped GaN with a low energy electron beam. The problems involved with obtaining controlled, reproducible p-type doping in GaN are presently challenging. In contrast, field effect transistors are majority carrier devices that do not suffer from minority carrier lifetime problems, and can be made with a material that only affords one type of mobile carrier. In fact, Asif Khan and co-workers have recently announced the first demonstration of a GaN metal semiconductor field effect transistor (MESFET).<sup>15</sup> They deposited 600 nm of unintentionally doped n-type GaN on an AlN buffer layer using a (0001) sapphire substrate. The n-type GaN formed the conducting channel for this MESFET. With a carrier concentration of  $1 \times 10^{17} \text{ cm}^{-3}$ , the channel was completely depleted at a reverse bias of -12V on the gate (a Schottky barrier formed with a silver electrode). The measured and calculated<sup>16</sup> transconductance of about 20 mS/mm was found to be consistent with a saturated drift velocity under the gate of  $5 \times 10^6 \text{ cm/s}$ . This work forms the basis for the establishment of high temperature electronic devices based on GaN.

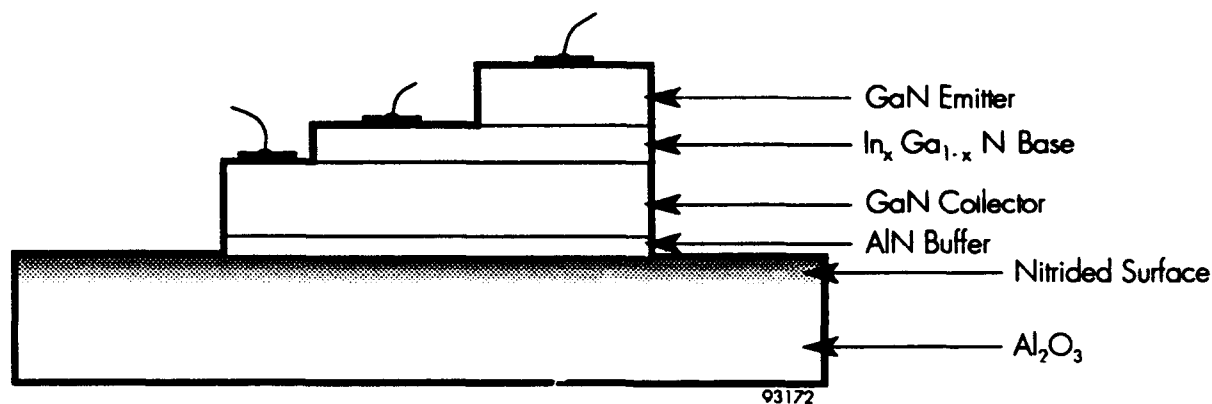


**Figure 3** *Spire's concept of a high temperature HBT based on GaN-InN alloys.*

Asif Khan and co-workers have now also produced a new *high electron mobility transistor* (HEMT) based on a two dimensional electron gas situated at a GaN- $\text{Al}_x\text{Ga}_{1-x}\text{N}$  heterojunction.<sup>17</sup> Once again using a sapphire substrate overcoated with an AlN buffer layer, they deposited a 600 nm n-type GaN channel with a 100 nm n-type  $\text{Al}_{0.14}\text{Ga}_{0.86}\text{N}$  cap layer, as shown in Figure 4. The transconductance of the device was measured to be 28 mS/mm. This transconductance is about a factor of ten lower than present day HEMTs based on GaAs or InP materials.<sup>18,19</sup> The basic problem appears to be the high level of background doping in the nitride layers, which is at the  $1 \times 10^{18} \text{ cm}^{-3}$  level.<sup>20</sup> However, the results clearly show the feasibility of producing FETs based on GaN.

### 2.3 Alternative Nitride Materials for Transistor Applications

The HEMT reported by Khan was based on using  $\text{Al}_x\text{Ga}_{1-x}\text{N}$  as the electron source for the two dimensional gas which resides in the GaN at the heterojunction.<sup>17</sup> Unfortunately, the aluminum alloys are more difficult to make in conducting form, and in fact, for alloys approaching 30% Al, the resistivity is about  $10^4 \Omega\text{-cm}$ .<sup>21</sup> Thus making electrical contacts to devices based on  $\text{Al}_x\text{Ga}_{1-x}\text{N}$  poses a problem. Therefore,  $\text{Al}_x\text{Ga}_{1-x}\text{N}/\text{GaN}$  heterojunctions may not be the best approach for fabricating high temperature transistors. An alternative strategy can be based on nitrides featuring bandgaps which are smaller than GaN. In such a case, the electron source would originate in the GaN, while the resulting two dimensional electron gas would be confined in the nitride alloy with the smaller bandgap.

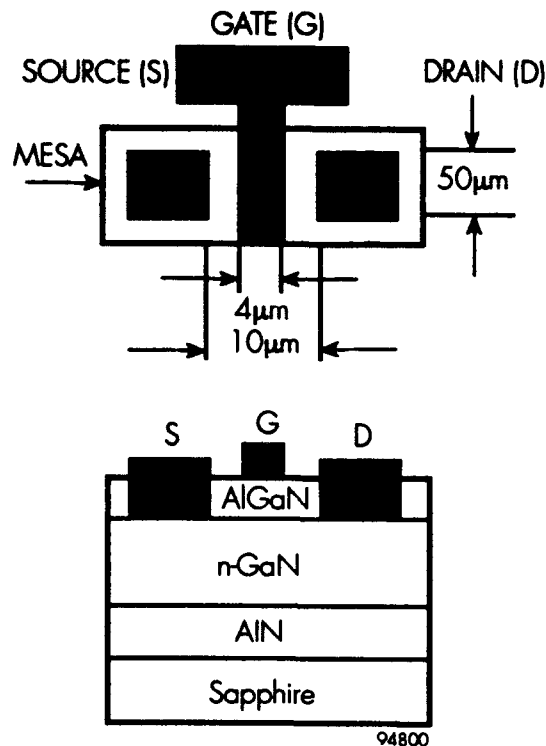


**Figure 4** Plan and cross-sectional view of fabricated HEMT.

It appears that  $\text{In}_y\text{Ga}_{1-y}\text{N}$  alloys may provide the ideal solution to the problem. Tansley and Foley<sup>22</sup> have prepared  $\text{InN}$  films with mobilities as high as  $2700 \text{ cm}^2/\text{V-s}$  at room temperature, a far higher value than ever found for  $\text{GaN}$  or  $\text{AlGaIn}$ . Thus a  $\text{GaN}/\text{InGaIn}$  HEMT would be analogous to  $\text{InP}/\text{InGaAs}$  HEMTs, which prove to be very fast due to the high mobility of  $\text{InGaAs}$ .<sup>23</sup> The bandgaps of  $\text{GaN} - \text{InN}$  alloys span the energy region from 3.4 to 1.9 eV, so confinement of the electron gas by a potential barrier should not be a problem even for low  $\text{In}$  concentrations. Although  $\text{InN}$  is not lattice matched to  $\text{GaN}$ , alloys with low  $\text{In}$  concentrations may prove useful, especially if a sapphire substrate is used for the deposition, since buffer layers can alleviate the mismatch problems.<sup>24</sup>

A relatively unexplored material which may fit the description for a low bandgap partner for  $\text{GaN}$  is  $\text{ZnGeN}_2$ , a semiconductor also first reported as an epitaxial thin film by Maruska.<sup>25</sup> In these early efforts, Maruska used elemental zinc and elemental germanium pellets held in two boats in a tube furnace; he transported them to the reaction zone as their chlorides. The films were deposited onto basal plane sapphire substrates, and optical absorption studies indicated that the material has a bandgap of about 2.7 eV.  $\text{ZnGeN}_2$  is very closely lattice matched to  $\text{GaN}$ . It is pseudo-hexagonal, with lattice parameter  $a = 3.193 \text{ \AA}$ . It can therefore be expected that  $\text{ZnGeN}_2/\text{GaN}$  heterojunctions may operate in the same manner as  $\text{AlGaAs}/\text{GaAs}$  heterojunctions.

There are only a few reports on the deposition or properties of  $\text{ZnGeN}_2$ . Maunaye et Lang<sup>26</sup> prepared  $\text{ZnGeN}_2$  by reacting zinc metal with  $\text{Ge}_3\text{N}_4$  at  $750^\circ\text{C}$ . Their product was contaminated with excess  $\text{Ge}$ . Very recently, Endo *et al.*,<sup>27</sup> mixed  $\text{Zn}_3\text{N}_2$  with either  $\text{Si}_3\text{N}_4$  or  $\text{Ge}_3\text{N}_4$  powders and heated them at 1000 to  $1600^\circ\text{C}$  under an extremely high pressure of 4 to 6.5 GPa for several hours. They report recovering both  $\text{ZnGeN}_2$  and  $\text{ZnSiN}_2$ . For  $\text{ZnSiN}_2$ , they determined the lattice parameter  $a = 3.035 \text{ \AA}$ , indicating that quaternary alloys would have a

smaller lattice parameter than  $\text{ZnGeN}_2$ . Endo's samples of  $\text{ZnGeN}_2$  were black and conducting, probably due to a lack of stoichiometry (nitrogen loss during the reaction). Grekov *et al.*, have presented a detailed discussion of the structure and chemical bonding in ternary nitrides.<sup>28</sup>  $\text{ZnGeN}_2$  has the sodium  $\beta$ -ferrite rhombohedral structure, the hexagonal equivalent of cubic chalcopyrite. The cations, Zn and Ge, are ordered in the  $\text{ZnGeN}_2$  structure.<sup>29</sup> Ordering of the cations is accompanied by deviations from the ideal atomic positions of wurtzite.  $\text{ZnGeN}_2$  exhibits significant rhombic expansion, and therefore may be a potentially useful material for non-linear optical effects.

Because our results with  $\text{In}_x\text{Ga}_{1-x}\text{N}$  have been so promising, we did not pursue the deposition of  $\text{ZnGeN}_2$ .

## 2.4 Plasma Assisted Deposition of Nitrides

Most films of GaN are highly conducting, with n-type carrier concentrations as high as  $1 \times 10^{20} \text{ cm}^{-3}$ . The donors have recently been clearly identified as nitrogen vacancies.<sup>30</sup> The basic problem with nitride growth is that ordinarily Ga compounds do not react with  $\text{N}_2$  gas, requiring that  $\text{NH}_3$  be used as the nitrogen precursor. However, because of the great stability of the N-N bond, much of the nitrogen associated with the ammonia becomes tied up as  $\text{N}_2$  in any common reaction chamber. Consequently, the growth and decomposition of GaN occur simultaneously on the growing surface, leading to the incorporation of vacant nitrogen sites in the film.

It is clearly advantageous to provide a more active source of N than ammonia. For example, good results have been reported for GaN films grown by electron cyclotron resonance (ECR) microwave plasma assisted molecular beam epitaxy.<sup>31</sup> The films were grown by the reaction of Ga vapor with ECR-activated nitrogen. This study found that at low microwave power levels, insufficient atomic nitrogen was transported into the reaction chamber, and gallium droplets formed on the sapphire substrate. Higher concentrations of atomic nitrogen lead to more insulating GaN films. The first report of plasma assisted MOCVD of GaN was presented by Zembutsu and Sasaki in 1986.<sup>32</sup> However, their films were just as highly conducting as GaN grown from ammonia. It appears to be very difficult if not impossible to obtain films of InN unless a source of atomic nitrogen is available; without the use of a nitrogen plasma, only droplets of indium metal are obtained in an MOCVD reactor.<sup>33</sup> However, using a nitrogen plasma source, single crystal InN films have been deposited on sapphire substrates at temperatures below  $500^\circ\text{C}$ .<sup>34</sup>

In order to prepare nitride films with sufficient quality for high temperature transistors, we have concluded that an ECR plasma source of nitrogen will be very beneficial. Therefore, conditions for adding such a plasma to an MOCVD reactor have been established as part of this program. The major advantages of plasma-assisted CVD are that a) microwave heating of gaseous reactants increases the internal energy of reactive species, leading to lower growth temperature requirements, and that b) non-reactive or low reactivity molecules may be dissociated into highly reactive species. ECR plasmas, in particular, have the proven advantages of high ionization efficiency, high plasma density and operation over a wide pressure range. The high plasma density results in a high efficiency for the dissociation of the gas molecules, and consequently a high deposition rate. The lifetime of the excited species tends to be long when

the operating pressure is kept low. These considerations are particularly important for the deposition of the nitrides, because basically the  $N_2$  molecule fails to combine with indium, gallium, or aluminum under standard conditions; thus the reaction,



effectively competes with the desired reaction for forming In, Ga, or AlN. A plasma source of  $N^+$  provides a great advantage over purely thermal activation of ammonia.

### 3 EXPERIMENTAL RESULTS AND DISCUSSION

#### 3.1 Development of ECR-Plasma Assisted MOCVD of Nitrides

The ECR plasma reactor is shown in Figure 5. The nitrogen plasma is generated in the center section of the reactor, where all of the magnets are located. Ultra high purity  $N_2$  serves as the source of nitrogen for the plasma. Microwaves are generated with a magnetron tube. The output from the magnetron is connected to a circulator and then to a dual directional coupler. For better transmission, waveguide coupling between the microwave system and the chamber is used. The microwave power is controlled by changing the current through the magnetron and monitored by the crystal detector mounted on the directional coupler. The microwaves enter the chamber from the right side, as shown.

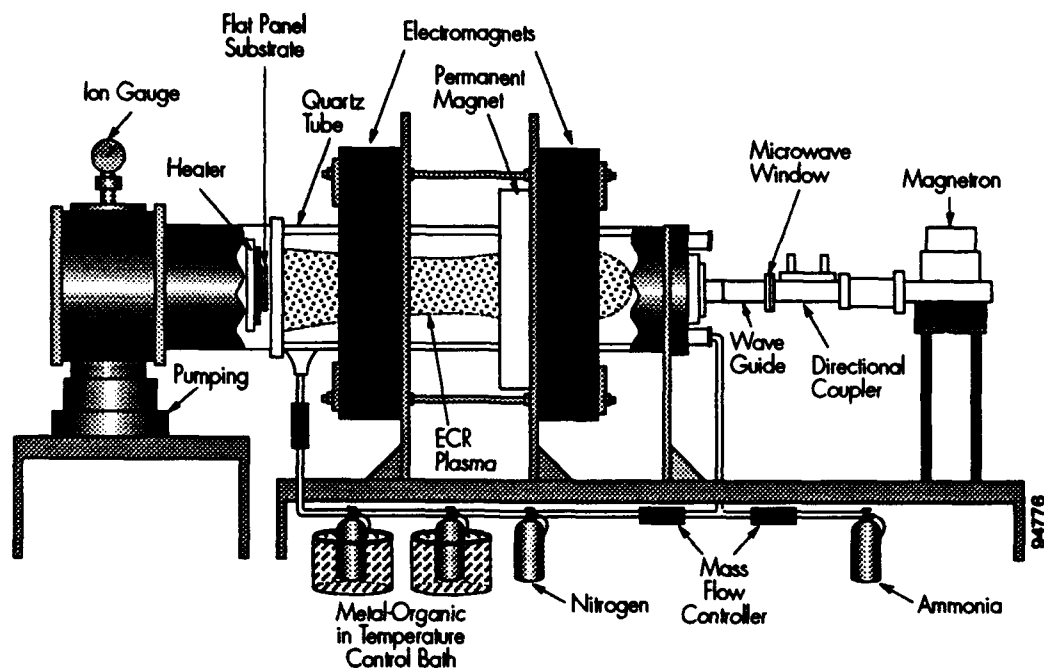


**Figure 5** *Spire's ECR plasma source modified as a crystal growth reactor.*

The substrate for the film deposition is mounted on a sample holder which is electrically insulated from the chamber. The sample holder is placed at the left side of the reactor, just outside the region in which the plasma is generated. There is a heater mounted on the back of the substrate so that its temperature can be externally controlled. By changing the distance between the substrate and the ECR zone, the plasma heating effect can be varied. Substrate temperature is monitored by an AC thermocouple. Crystalline sapphire substrates were placed on the sample holder in the ECR plasma reactor for all depositions that were undertaken this month; these transparent substrates are very useful for ease of optical evaluation.

A cylinder filled with trimethylgallium was connected to the reactor with stainless steel tubing. The metalorganic gas flow is regulated by a stainless steel needle valve. The TMG enters the reaction zone in the chamber through a stainless gas ring. At the same time a gas flow controller regulates the nitrogen flow to maintain the chosen operating pressure over the range  $10^{-5}$  to 1 torr.

There are five important parameters affecting the quality of crystal growth in Spire's ECR plasma reactor: the substrate temperature, the source gas constituents, the gas pressure, the microwave power, and the magnetic field. Each of the five parameters must be considered in a matrix configuration of experimental conditions in order to optimize the growth conditions. Thus a considerable number of depositions will be required in order to obtain the best quality films. At this time, we have just begun to vary some of these parameters in our reactor.

### 3.2 Experimental Conditions for GaN Deposition

The key factor in these experiments was the generation of sufficient concentration of active nitrogen species to allow the growth of stoichiometric GaN films. High purity nitrogen gas from a cylinder was fed into the vacuum chamber through stainless steel tubing, a shut-off valve, and a pressure valve operated by a pressure controller. Microwaves at 2.45 GHz were conducted into the chamber which features both permanent and electromagnets. The nitrogen plasma is therefore generated by electron cyclotron resonance heating of the nitrogen gas.

Trimethylgallium (TMG) was introduced into the growth chamber through a stainless steel "shower ring" gas injector, shown in Figure 6. The sample holder is located directly in front of the gas injector. The flow rate of TMG is controlled with a needle valve. The TMG bubbler is held at room temperature. No carrier gas is passed through the TMG bubbler.

Sapphire substrates were cleaned in the manner to be described in Section 3.6.1. The sapphire wafers were each positioned (one per run) on the top of a specially designed resistive heater stage, supported by an aluminum fixture. The sample temperature was monitored by a thermocouple probe.

The nitrogen pressure in the chamber has been fixed at  $2 \times 10^{-4}$  torr. The V/III (N/Ga) ratio was varied by changing the TMG flow rate. Samples were grown at substrate temperatures from 250 to 800°C.

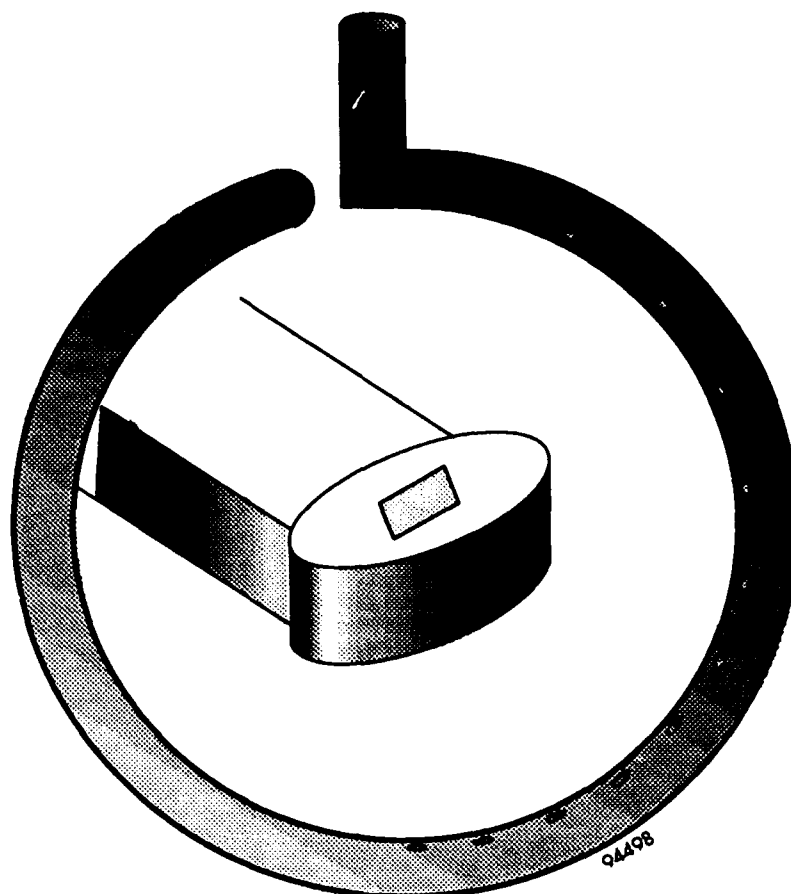


**Figure 6** *Showerhead gas injector.*

After the reactor was placed in operation, we began attempts to grow GaN. Our first three attempts were totally unsuccessful because our gas flowrates were far too low. This happened because we had positioned a metal screen between the main plasma chamber and the substrate, to prevent undesirable ionic bombardment of the film. There was no evidence of any deposit on the transparent substrate for the first three runs. The screen was then removed, and with the TMG pressure set above  $2 \times 10^{-6}$  torr, GaN films were prepared.

### 3.3 Properties of GaN Films

A total of nine GaN samples were attempted in the new ECR plasma assisted MOCVD reactor. The growth conditions are summarized in Table I.

The sample which demonstrated the best X-ray diffraction results was #6. This film was 250 nm thick, and proved to be a single crystal, oriented with (0002) planes parallel to the (0001) surface of the sapphire substrate. The diffraction pattern is shown in Figure 7. The absorption spectrum of sample #4 is shown in Figure 8. Notice the excellent characteristics of this film, with a sharp absorption edge at 365 nm, the known bandgap of GaN. Finally, the surface of sample #7 is shown in Figure 9. These sample are quite transparent and have specular surfaces.

**Table I** Growth conditions for ECR plasma assisted MOCVD of GaN.

Sample	TMG Pressure $\mu$ torr	V/III ratio	Substrate Temperature $^{\circ}$ C	Orientation	R, $k\Omega/\square$	Remarks
1	0.8	250	560		-	No deposit
2	0.5	400	400		-	No deposit
3	2.5	80	630		-	No deposit
4	2.0	100	660	Tilt	14	Thin film
5	3.3	60.6	630	Tilt	-	Smooth and clear
6	3.3	60.6	860	Flat	58	Smooth and clear
7	4.5	44.4	630	Flat	5	Smooth and clear
8	3	66.6	250	Tilt	$\infty$	Smooth and clear
9	3	66.6	350	Tilt	$\infty$	Smooth and clear

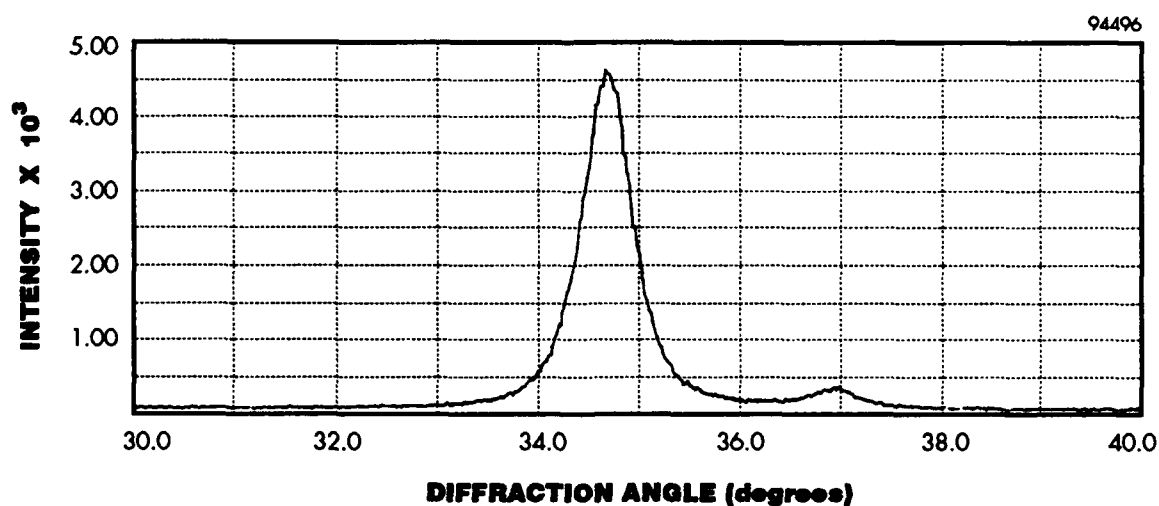


**Figure 7** X-ray diffraction pattern of plasma assisted GaN, indicating an epitaxial single crystalline film.



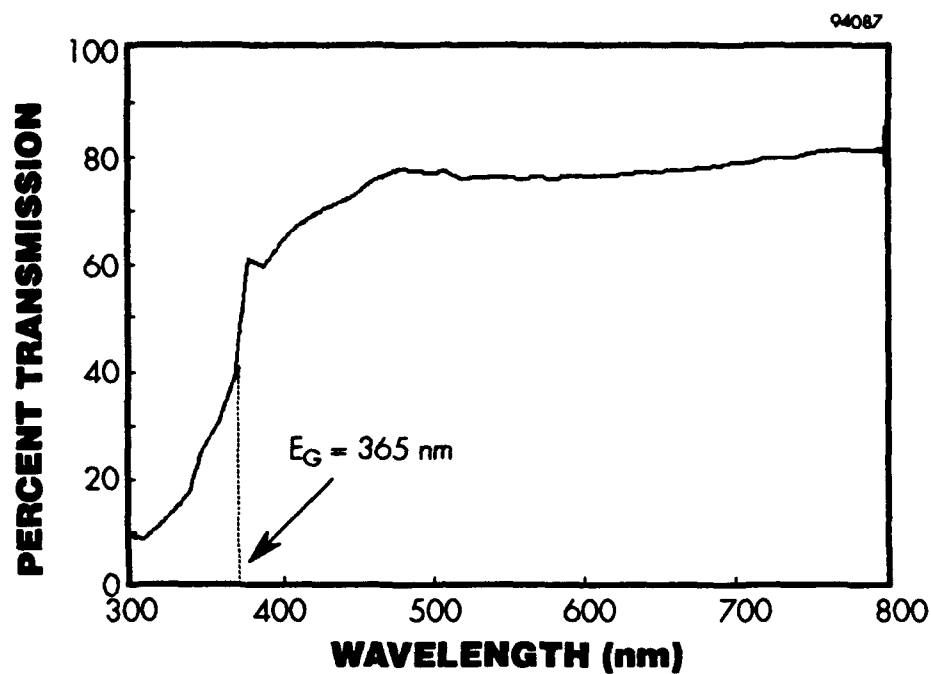


**Figure 8** *Absorption spectrum of plasma assisted GaN film, showing sharp absorption edge at 365 nm.*



**Figure 9** *Photomicrograph of the surface of a GaN film prepared in the plasma assisted MOCVD reactor.*

### 3.4 Development of ECR-Plasma Assisted MOCVD of Indium Nitride

A bubbler filled with TMI was hooked up to the same input line for the shower-head injector as the TMG is located. No carrier gas was supplied for the TMI, and it was expected that it would be transported by its own vapor pressure.

Initial runs attempted to establish optimum TMI flows and substrate temperatures required for deposition. The experimental parameters are given in Table II.

**Table II** *Growth conditions for ECR plasma assisted MOCVD of InN and  $\text{In}_x\text{Ga}_{1-x}\text{N}$ .*

Sample	Nitrogen Pressure $\mu\text{torr}$	TMG Pressure $\mu\text{torr}$	TMI Pressure $\mu\text{torr}$	V/III ratio	Substrate Temp. $^{\circ}\text{C}$	Remarks
11	400	0	20	20	630	Red deposit
12	400	0	10	40	630	Red deposit
13	400	0	6	66	400	Red deposit
14	400	0	15	26	300	Red deposit
15	200	0	10	20	300	Red deposit
16	200	0	8	25	300	Red deposit
17	200	3.9	2.4	32	630	Yellow deposit
18	150	6.3	1.3	26.6	630	Orange deposit
19	200	0	1.8	111	300	Dark orange
20	400	0.6	2.5	125	300	Dark orange

These experiments indicated that higher  $\text{N}_2$ :TMI ratios produced better films, but at the cost of lower TMI flows, and hence lower growth rates. An example of this effect is shown in Figure 10. Higher substrate temperatures resulted in black films, probably from thermal decomposition of TMI on the substrate with consequent carbon incorporation into the films. This is shown in Figure 11.

Even with optimized TMI flow and substrate temperature, the measured absorption edges were not abrupt. Elemental analysis by Auger electron spectroscopy revealed significant oxygen incorporation into the films with slightly lower oxygen content in those films which were deposited with both cryopump and turbopump than in films deposited with the turbopump alone. This is shown in Figure 12.

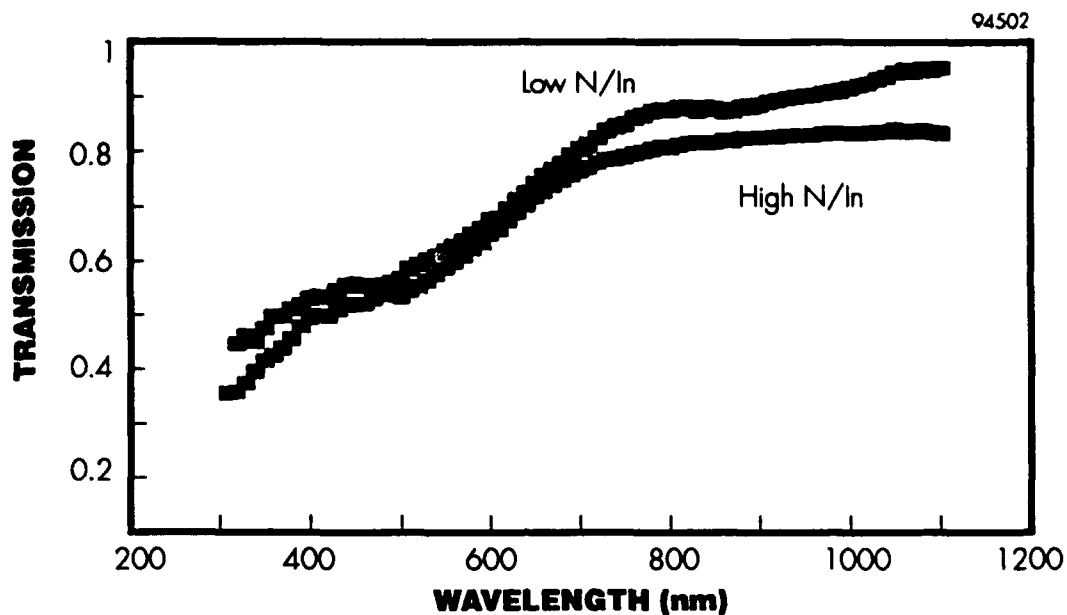


**Figure 10** *Growth of InN by PA-MOCVD: better films result at larger N/TMI flow ratio.*

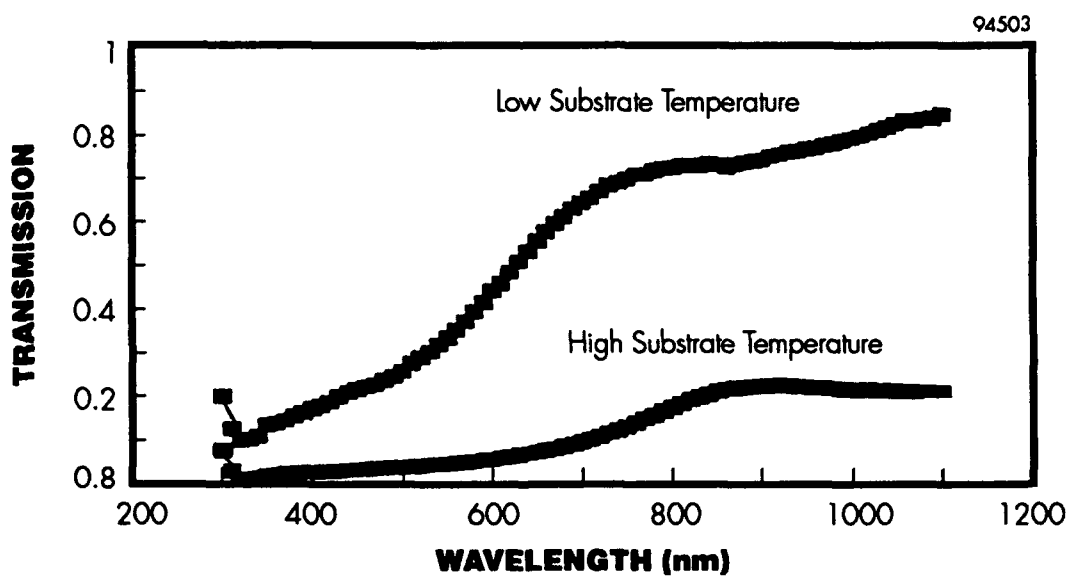


**Figure 11** *High growth temperatures apparently pyrolyze the TMI, introducing carbon contaminants.*

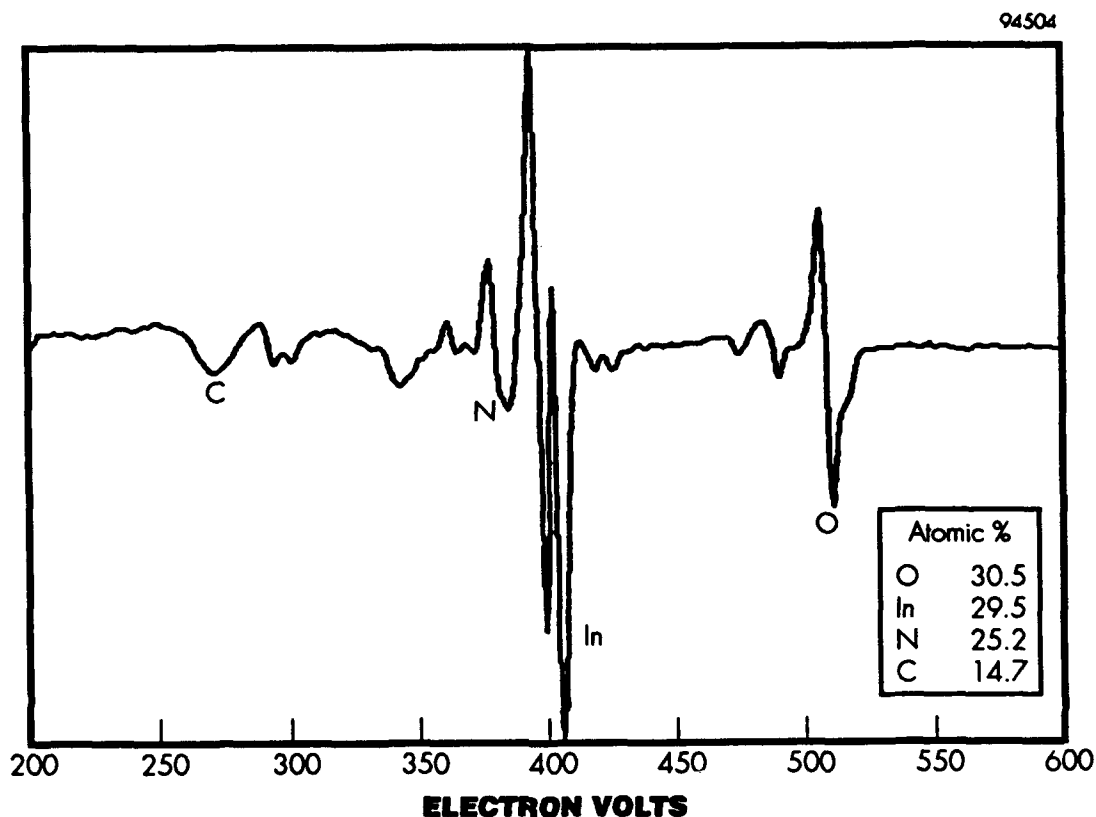


**Figure 12** Auger electron spectroscopy of InN film.

We then introduced both TMI and TMG into the reactor in order to prepare  $\text{In}_x\text{Ga}_{1-x}\text{N}$  alloys. Several films were deposited with varying ratios of TMI and TMG; details of the growth conditions for samples #17 and #18 were listed in Table II. Optical transmission measurements showed that it is indeed possible to control the absorption edge, shifting the onset of absorption through the visible spectrum, as shown as an example in Figure 13. The Auger analysis shown in Figure 14 clearly indicated the presence of both gallium and indium in these alloy films.

To reduce the oxygen content, several modifications were made to the growth apparatus. The TMI bubbler was replaced with a second bubbler, along with its stainless steel gas line and needle valve. To monitor the residual gas and diagnose possible problems, a residual gas analyzer (RGA) with attached vac-ion pump was mounted on the chamber. Since the RGA is several orders of magnitude more sensitive than a helium leak checker, it was used to re-check the entire chamber and gas supply system for leaks to atmosphere. This procedure identified two very small leaks ( $10^{-12}$  torr) which were repaired, but no significant atmosphere leaks. It was concluded that oxygen contamination may be inherent to the present reaction vessel, especially since the chamber is fabricated from aluminum.

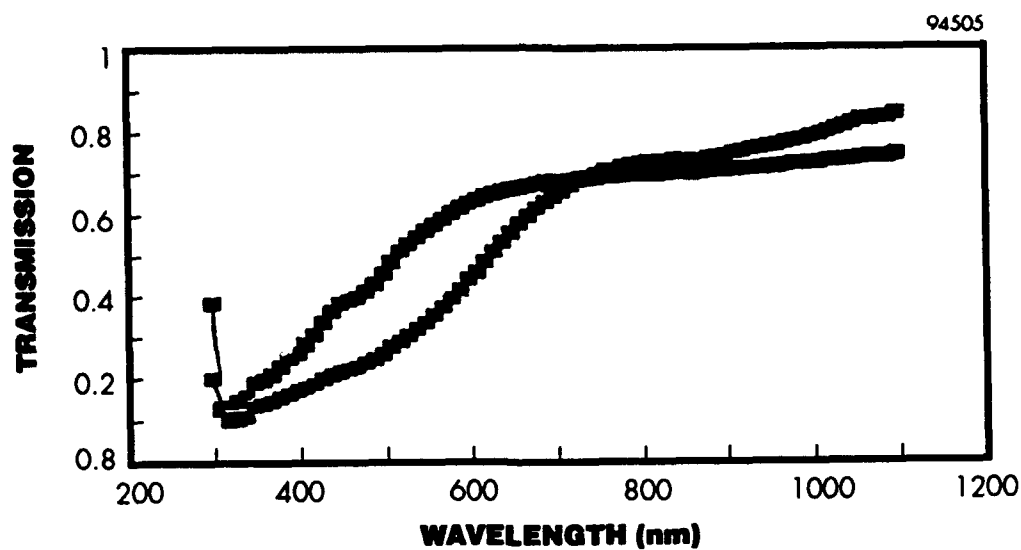


**Figure 13** *Varying Ga:In ratio shifts the absorption band edge.*

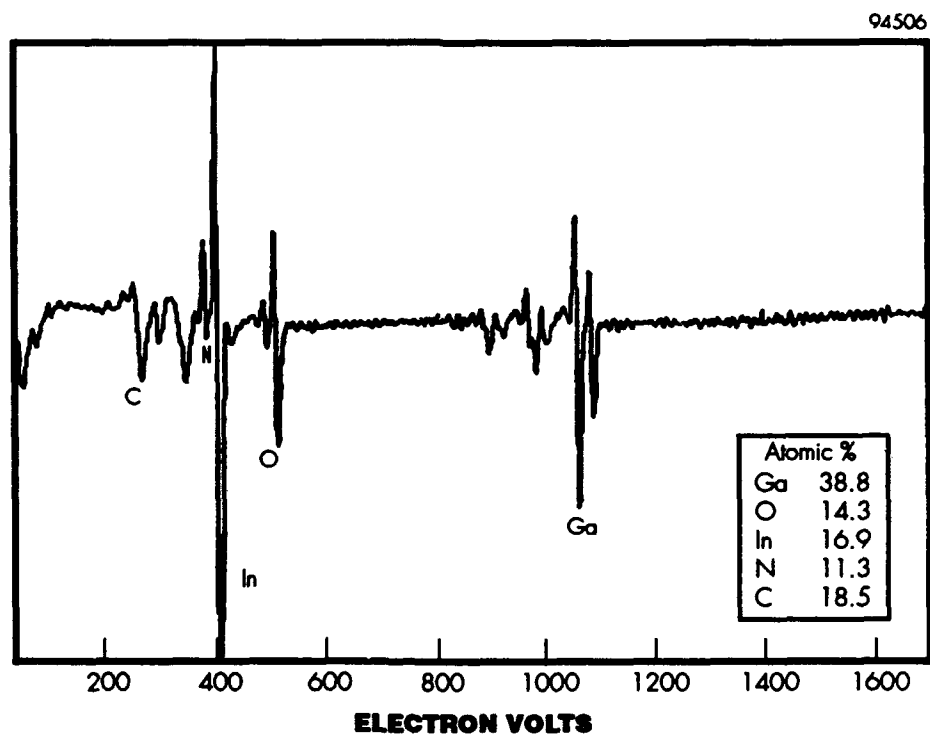


**Figure 14** *Auger electron spectroscopy of  $\text{In}_x\text{Ga}_{1-x}\text{N}$  film.*

### 3.5 Optical Absorption Studies

Measurements of the optical transmission  $T$  as a function of probe light wavelength  $\lambda$  were undertaken for all of the samples. Using such data, we calculated the absorption constant  $\alpha$  vs. energy for a sample of InN, a sample of  $\text{In}_x\text{Ga}_{1-x}\text{N}$  with a low Ga concentration, a sample of  $\text{In}_x\text{Ga}_{1-x}\text{N}$  with high Ga content, and pure GaN. Basically,

$$T(\lambda) = I(\lambda)/I_0 = \exp(-\alpha(\lambda)d) \quad (2)$$

where  $I_0$  is the calibrated input intensity of the probe light,  $I$  is the intensity of the light which is transmitted through the film, and  $d$  is the thickness of the film (measured separately). Thus we calculated  $\alpha$  from the transmission data using equation (2). For a direct bandgap material, it is expected that,<sup>1</sup>

$$\alpha = \alpha_0(E - E_g)^{0.5} \quad (3)$$

Therefore, we plotted the square of the absorption constant vs. energy. The results were presented in Figure 1 in the Summary section. Almost all of the data points for any of the samples fit readily to a straight line. Thus we are confident that the materials possess a direct bandgap. From the intercept of the lines with the energy axis, we find that for InN,  $E_g = 1.92$  eV, while the alloys had bandgaps of 2.12 and 2.7 eV. GaN had a bandgap of 3.38 eV. Therefore, we have definitely increased the bandgap of InN by alloying with Ga.

These results are similar to those reported by Osamura *et al.* for InN, GaN and InN-GaN alloys in 1972.<sup>2</sup> They prepared their films by passing a nitrogen plasma over a boat filled with a liquid mixture of indium and gallium metals. Their data points all clearly fit a straight line in their plot of  $\alpha^2$  vs.  $E$ . According to their data, they interpreted the bandgap of InN to be 1.9 eV, and that of GaN to be 3.4 eV. Therefore, our results are perfectly consistent with this older report.

### 3.6 Summary of Initial Work on Standard MOCVD of GaN

In the early efforts in this program, we attempted to deposit GaN films in a standard MOCVD reactor using trimethylgallium and ammonia as the reactants. Because the films had inadequate quality, this approach was abandoned in favor of the PA-MOCVD method. Standard MOCVD also appears to lack the nitrogen activity required to produce  $\text{In}_x\text{Ga}_{1-x}\text{N}$  alloys. The following sections serve to summarize these efforts, which we do not expect to pursue any further.

#### 3.6.1 Basic Growth Parameters

The following starting conditions were established for the deposition of GaN in the conventional MOCVD reactor.

**Sapphire Substrate** - Hot etch for 15 minutes in 1:3  $\text{H}_3\text{PO}_4:\text{H}_2\text{SO}_4$ . Preheat substrate to 1150 to 1200°C in 1 slm of hydrogen to clean the surface.

**Ammonia Flow Rate** - We have installed a new ammonia flow controller that can handle up to 5 lpm gas flow. This should be sufficient to provide the desired ammonia flow over the sample.

**Buffer Layer** - According to the literature, the temperature for the buffer should be in the range of 450 to 600°C.<sup>35</sup> Hydrogen flow of 2.5 slm. Trimethyl gallium (TMG) should be about 10 to 50  $\mu$ moles/minutes. Ammonia flow should be about 1 to 2 lpm. Buffer growth time less than 10 minutes. Expected that film should be about 200Å thick.

**Emitter Layer** - Temperature of 1000 to 1100°C. Hydrogen 3.5 slm. Ammonia 1500 sccm. TMG 3 to 10 sccm at 10°C.

### 3.6.2 GaN Crystal Growth

A graphite foil liner was installed in the furnace to prevent deposition of nitrides on the walls of the quartz tube. The system pressure was set to 70 torr, with an argon flow of 2000 sccm. The furnace temperature was raised to 1000°C, the tube was baked for 20 minutes, and then allowed it to cool down in flowing nitrogen overnight.

Three 1 cm<sup>2</sup> sapphire substrates were etched as described above and rinsed with deionized water before being loaded in the furnace. The temperature was raised to 1000°C with hydrogen flowing at 3350 sccm. The ammonia flow was set at 1650 sccm. The TMG was held at 23°C, as were the TMG input lines. A flow of 3 sccm H<sub>2</sub> was set through the TMG. The samples were heated for 0.25 hour in hydrogen at 1000°C. The furnace was then cooled to 850°C and the TMG was turned on to grow a GaN buffer layer for 10 minutes. The NH<sub>3</sub> was kept flowing at all times. The temperature of the furnace was raised back up to 1000°C to grow the final GaN layer for 30 minutes.

A second set of samples was subsequently grown. To reduce the thickness of the deposits, we tried to reduce the gallium flow by cooling it with cold water. The water temperature was 17°C. The gallium input line remained at 21°C. The NH<sub>3</sub> flow once again was 1650 sccm, while the hydrogen flow was 3350 sccm. The system was pumped down to about 0.3 torr and then back filled with hydrogen. The samples were held at 1000°C for 15 minutes, with the sample holder placed at the downstream end of the tube. When the deposition was over, the samples were cooled down in flowing N<sub>2</sub> + NH<sub>3</sub>.

### 3.6.3 GaN Characterization

The substrates from the first run were coated with a dark material. The coatings were very thick and somewhat conducting ( $> 50\Omega$ ) and tended to peel off the substrates. Photoluminescence was checked with a mercury lamp emitting at 254 nm, but no visible light emission was observed. The optical transmission of a particular sample is shown in Figure 15. The drop in transmission between 300 and 400 nm is characteristic of GaN.

An Auger analysis was performed on this film, and is shown in Figure 16. The C line is due to inadvertent surface contamination with hydrocarbons. The Al and O peaks are from the sapphire substrate. The fact that the Ga peak is stronger than the N peak may indicate contamination of the film with elemental Ga.

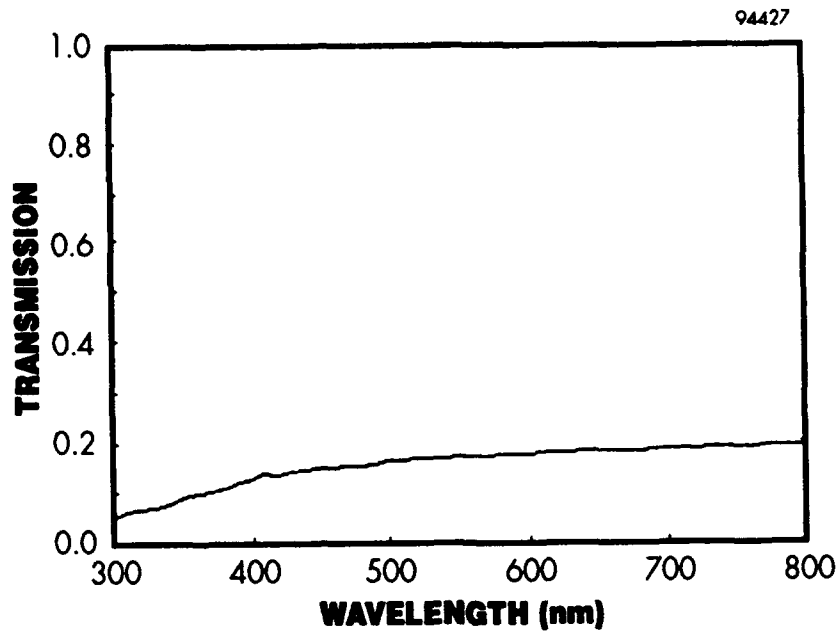


**Figure 15** *Optical transmission spectrum of GaN sample grown by conventional MOCVD.*

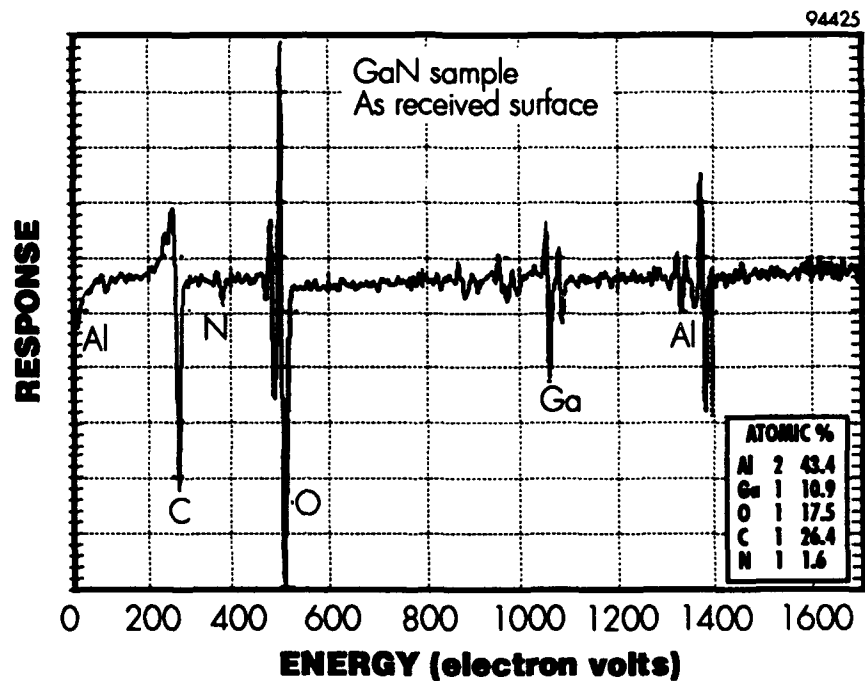


**Figure 16** *Auger analysis of GaN sample.*



The three samples from the second growth run were also characterized. One sample was found to have a very even frosty white haze on it. The other samples had a thicker deposits and were darker in color. Photoluminescence was studied with the 254 nm output of the mercury vapor lamp. The frosty white sample glowed bright orange, while the other samples showed no visible photoluminescence. These films showed no measurable electrical conductivity.

The frosty white sample was characterized by X-ray diffraction. The result is shown in Figure 17. Measurements were made on the front and the back of the sample. Either surface exhibited strong peaks corresponding to crystalline sapphire at  $d = 2.16$  and  $d = 2.58\text{\AA}$ . The significant difference for the grown film side was a relatively strong extra peak at  $2.42\text{\AA}$ . Such a peak can be indexed as the (101) line of GaN. However, the test indicates that the sample is basically a random textured (polycrystalline) film of GaN.

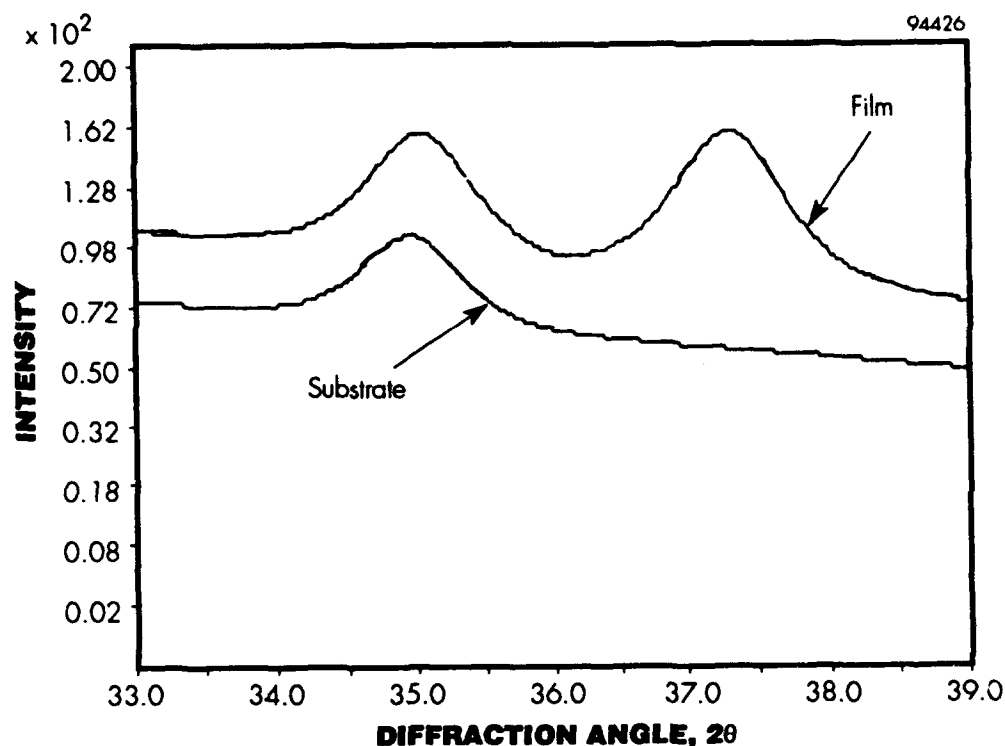


**Figure 17** X-ray diffraction analysis of GaN sample #11, indicating (101) peak of GaN.

#### 4 ANALYSIS OF RESULTS AND RECOMMENDATIONS

We have successfully converted an MOCVD reactor to supply a nitrogen plasma for growing nitrides. We have determined that InN is as readily grown as GaN in our PA-MOCVD reactor. We have been able to demonstrate shifting of the absorption edge from 1.9 eV to 3.4 eV as Ga was added to the In in the reactant stream. The optical absorption spectra indicated direct bandgap materials. This is a very positive finding, because we are now in a position to form heterojunctions between GaN and  $\text{In}_x\text{Ga}_{1-x}\text{N}$  which can serve as either an emitter/base combination for an HBT, or a spacer/channel for a HEMT.

However, the absorption edge of InN and In-rich alloys is not sharp enough, indicating the probable presence of impurities such as oxygen. The Auger characterization indicated only oxygen as a major impurity. Although there were no identifiable leaks in the chamber, we suspect that the plasma may be liberating oxygen that is either adsorbed or present as  $\text{Al}_2\text{O}_3$  on the walls of the aluminum reaction chamber. This problem needs to be remediated, basically by replacing the aluminum chamber with a new one based on a more robust material such as stainless steel.

To overcome virtual leaks and getter residual gas adsorbed onto the chamber walls, a titanium sputter source can be mounted to the sample stage and external heaters could be mounted to the chamber walls. The cryopump could be upgraded with an integral on-board controller and externally controlled throttle valve. The throttle valve would be particularly significant because it will allow higher pressure operation with carrier gasses for the gallium and indium sources. These changes should produce a significant improvement in the water and oxygen residual gas background in the vacuum chamber.

The GaN films proved to be highly oriented single crystals matched to the (0001) planes of the sapphire substrates. More work will be necessary for characterizing the alloys. The use of other sapphire orientations may prove to be beneficial in improving crystallinity. It will also be necessary in future work to perform a detailed study of film conductivity vs. nitrogen activity in the reactor.

For a Phase II program, we suggest that initial work should concentrate on perfecting the GaN films and providing controlled doping of such films. Buffer layers need to be studied. Work should then turn to perfecting the structure and purity of the alloy materials, and doping studies should be commenced. GaN/ $\text{In}_x\text{Ga}_{1-x}\text{N}$  heterojunctions need to be characterized. When the materials properties have been optimized, we will be able to fabricate transistor structures, and to provide extensive characterizations of their operating characteristics.

## 5 REFERENCES

1. R.A. Smith, *Semiconductors*, Cambridge University Press, p.193-211, 1968.
2. K. Osamura, K. Nakajima, Y. Murakami, *Solid State Comm.*, **11**, 617 (1972).
3. H.P. Maruska and J.J. Tietjen, *Appl. Phys. Lett.*, **15**, 327 (1969).
4. J.I. Pankove, J.E. Berkeyheiser, H.P. Maruska, J. Wittke, *Solid State Comm.*, **8**, 1051 (1970).
5. J.I. Pankove, H.P. Maruska, J.E. Berkeyheiser, *Appl. Phys. Lett.*, **17**, 197 (1970).
6. H.P. Maruska, W.C. Rhines, D.A. Stevenson, *Mat. Res. Bull.*, **7**, 777 (1972).
7. H.P. Maruska, D.A. Stevenson, J.I. Pankove, *Appl. Phys. Lett.*, **22**, 303 (1973).
8. H.P. Maruska and D.A. Stevenson, *Solid State Electronics*, **17**, 1171 (1974).
9. M.A. Khan *et al.*, *Appl. Phys. Lett.*, **42**, 430 (1983).
10. T. Kawabata *et al.*, *J. Appl. Phys.*, **56**, 2367 (1984).
11. H. Amano *et al.*, *Appl. Phys. Lett.*, **48**, 353 (1986).
12. H. Kroemer, *J. Vac. Sci. Technol.*, **B1**, 112 (1983).
13. W. Shockley, US Patent 2,569,347, (1951).
14. S. Nakamura, M. Senoh, T. Mukai, *Japanese J. Appl. Phys.* **30**, L1708 (1991).

15. M. Asif Khan, J.N. Kuznia, A.R. Bhattarai, D.T. Olsen, *Appl. Phys. Lett.*, **62**, 1786 (1993).
16. R.E. Williams and D.W. Shaw, *IEEE Trans. Electron Dev.*, **25**, 600 (1978).
17. M. Asif Khan, A. Bhattarai, J.N. Kuznia, D.T. Olson, *Appl. Phys. Lett.*, **63**, 1214 (1993).
18. R. Lai, M. Wojtowicz, C.H. Chen, M. Biedenbender, H.C. Yen, D.C. Streit, K.L. Tan, P.H. Liu, *IEEE Microwave and Guided Wave Letters*, **3**, 363 (1993).
19. A.M. Kusters, A. Kohl, R. Muller, V. Sommer, K. Heime, *IEEE Electron Device Lett.*, **14**, 36 (1993).
20. M. Asif Khan *et al*, *Appl. Phys. Lett.*, **60**, 3027 (1992).
21. S. Yoshida, S. Misawa, S. Gonda, *J. Appl. Phys.*, **53**, 6844 (1982).
22. T.L. Tansley and C.P. Foley, *Electron Lett.*, **20**, 1066 (1984).
23. H. Wang, R. Lai, S.T. Chen, J. Berenz, *IEEE Microwave and Guided Wave Lett.*, **3**, 381 (1993).
24. J. N. Kuznia *et al*, *J. Appl. Phys.*, **73**, 4700 (1993).
25. H.P. Maruska, W.L. Larson, and D.A. Stevenson, *J. Electrochem. Soc.*, **121**, 1673 (1974).
26. M. Maunaye and J. Lang, *Mat. Res. Bull.*, **5**, 793 (1970).
27. T. Endo, Y. Sato, H. Takizawa, M. Shimada, *J. Mater. Sci. Lett.*, **11**, 424 (1992).
28. F.F. Grekov *et al.*, *Inorganic Materials*, **15**, 1546 (1979).
29. M. Wintenberger, *Mat. Res. Bull.*, **8**, 1049 (1973).
30. T.D. Moustakas and R.J. Molnar, *Mat. Res. Soc. Symp. Proc.*, **281**, 753 (1993).
31. C.R. Eddy, T.D. Moustakas, J. Scanlon, *J. Appl. Phys.*, **73**, 448 (1993).
32. S. Zembutsu and T. Sasaki, *Appl. Phys. Lett.*, **48**, 870 (1986).
33. A. Wakahara, T. Tsuchiya, A. Yoshida, *J. Crystal Growth*, **99**, 385 (1990).
34. A. Wakahara and A. Yoshida, *Appl. Phys. Lett.*, **54**, 709 (1989).
35. J.N. Kuznia, M. Asif Khan, D.T. Olsen, *J. Appl. Phys.*, **73**, 4700 (1993).